Pergamon

Int. J. Heat Mass Transfer. Vol. 37, No. 15, pp. 2231–2244, 1994

0017–9310/94 $7.00+0.00

0017–9310(94)E0042–S

Laminar developing flow and heat transfer between a series of parallel plates with surface mounted discrete heat sources

S. H. KIM† and N. K. ANAND‡

Department of Mechanical Engineering, Texas A&M University, College Station, TX 77843-3123, U.S.A.

(*Received* 29 *September* 1993 *and in final form* 24 *January* 1994)

Abstract—Laminar developing flow (*DF*) and heat transfer between a series of conducting parallel plates (substrate) with surface mounted heat generating blocks were numerically studied with consideration given to flow of air ($Pr = 0.7$). These channels resemble cooling passages of electronic equipment. A single channel subjected to a repeated condition in the transverse direction was isolated as a computational domain. The governing equations were solved by a finite volume technique. The results of the *DF* problem were compared with the corresponding periodically fully developed flow (*PDF*) problem results and used to establish entry length. Thermal entry length decreased with an increase in substrate conductivity. Thermal performance of channels was characterized in terms of thermal resistance per unit length of the channel. To separate the effects of self heating and upstream heating for each module, thermal resistance based on the channel inlet temperature ($\bar{R}_o$) and module inlet bulk temperature ($\bar{R}_m$) was defined. These thermal resistances were correlated with the independent parameters such as the Reynolds number (Re), substrate thickness (t/w), block height (h/w), block spacing (s/w), channel height (d/w), and thermal conductivity ratio of the solid to fluid (K_s/K_f). The thermal resistance was found to decrease with an increase in Reynolds number, block spacing and substrate conductivity. The thermal resistance increased with an increase in the area of bypass flow ($1-h/d$), substrate thickness (t/w) and block height (h/w).

INTRODUCTION

COOLING of electronic components is crucial in maintaining operating temperature limit and peak performance. A number of thermal management strategies for electronic equipment are discussed by Nakayama [1] and Incropera [2]. Forced convection is one common way to cool channels with surface mounted chips. Heat transfer analysis of channels between circuit boards is challenging because of complex geometry, heating condition, and interaction between convection and conduction. Typical electronic equipment consists of a stack of circuit boards with a series of periodically surface mounted heat generating electronic chips. Air forced through channels formed between two adjacent circuit boards removes heat in part by forced convection while the rest is conducted to the substrate/circuit board and eventually dissipated in adjacent channels. This work studies laminar developing flow and heat transfer in such channels with the help of a two-dimensional model as shown in Fig. 1. Flow and heat transfer is periodically fully developed (*PDF*), far from the channel entrance. The scope of the present work is confined to the developing flow and heat transfer (*DF*) in the entrance region. Results of the *PDF* problem are reported elsewhere [3]. The study of developing flow and heat transfer will help understand the entrance effects and identify the onset of the *PDF* condition.

The objective of this work is to numerically study laminar developing flow and heat transfer between a series of parallel plates with five surface mounted heat generating blocks. The substrate conduction is included in the analysis and, thus, the channels are thermally linked to one another.

A small number of earlier investigations employed fairly simple models, consisting of a single parallel plate channel with a series of blocks on one side with either isothermal or isoflux heating conditions, e.g. ref. [4]. Experimental studies used the mass transfer technique by Sparrow *et al.* [5] and the heat transfer technique by Lehmann and Wirtz [6], Moffat *et al.* [7], Sridhar *et al.* [8], and Wirtz and Chen [9] to study turbulent heat transfer with surface mounted blocks in a single channel. All of these results represent the thermal characteristics of such channels, where walls were heated by subjecting them to uniform wall temperature or uniform heat flux along the entire length, or in part, of the channel. As pointed out by Incropera [2], Sathe and Joshi [10], Peterson and Ortega [11] conjugate effects play a very important role in cooling electronic chips. Conjugate effects have received con-

† Present address: Mechanical Engineering Department, Kei Myung University, Tae Gu, Korea.

‡ Author to whom correspondence should be addressed.

NOMENCLATURE

a	coefficients in discretization equation or correlation constants
b	correlation constants
c_p	specific heat
d	channel height
d_e	hydraulic diameter ($2d$)
DF	developing flow
f	friction factor
h	block height or heat transfer coefficient
K	thermal conductivity or iteration number
l	module length
l_b	inlet buffer length
N	block/module number
Nu	Nusselt number
Pr	Prandtl number
p	pressure
PDF	periodically fully developed flow
q	non-dimensional heat flux, $q''/Q'''h$
q''	dimensional heat flux
Q'''	heat source per unit volume per unit time
R	thermal resistance
Re	Reynolds number based on hydraulic diameter, $u_b d_e/\nu$
R_ϕ	residual in the discretization equations
s	spacing between blocks
S	source term
S_1, S_2	surface(s) where the repeated condition is imposed
T	temperature
t	substrate thickness
u	velocity in stream-wise direction
v	velocity in the transverse direction
x	stream-wise direction
y	transverse direction
z	distance along the bottom surface
w	block width.

Greek symbols

δ	Kronecker delta or distance between grid points
θ	non-dimensional temperature, $(T-T_0)/Q'''wh/k_f$
μ	dynamic viscosity
ν	kinematic viscosity
ρ	density
ϕ	general variable
ψ	stream function.

Subscripts

b	bulk or block
bot	bottom surface
f	fluid
i	interface
I	node index in x-direction
J	node index in y-direction
m	module
max	maximum
nb	neighborhood points
0	inlet
ref	reference
s	substrate or solid
w	wall
ϕ	general variable.

Superscript

$\bar{}$	average value or non-dimensional form.

siderable attention by several investigators [3, 12–17]. Davalath and Bayazitoglu numerically studied two-dimensional, steady laminar heat transfer between a series of parallel plates with surface mounted heat sources. Each channel had three heat sources. Stacking of parallel plates in the transverse direction was simulated by imposing the symmetric boundary condition ($\partial T/\partial y = 0$) for the temperature field midway between two adjacent plates while the natural boundary condition was imposed at the channel exit ($\partial T/\partial x = 0$). The present investigation differs from that of Davalath and Bayazitoglu [16] in the following ways: (1) a repeated condition [13] is adopted for the temperature field in the transverse direction to simulate stack of parallel plates; and (2) an alternative boundary condition (type-b) proposed by the authors [3, 18] is adopted for the temperature field at the channel exit. The model development, solution technique, validation of the solution technique and representative results are discussed in the following sections. Five heat generating blocks are considered in this investigation.

MODEL DEVELOPMENT

A two-dimensional, steady, laminar, developing flow and heat transfer between a series of parallel plates with five periodically surface mounted heat generating blocks in the entrance region is considered (Fig. 1a). Consideration is given to developing flow only. These channels resemble cooling passages of electronic equipment because the surface mounted blocks simulate electronic packages and the conducting plates simulate circuit board/substrates. The temperature field in each channel is thermally coupled because of wall conduction. However, due to geometrical symmetry, it is possible to confine the analysis to an interior single channel by employing repeated boundary condition on surfaces s_1 and s_2 (Fig. 1b) for

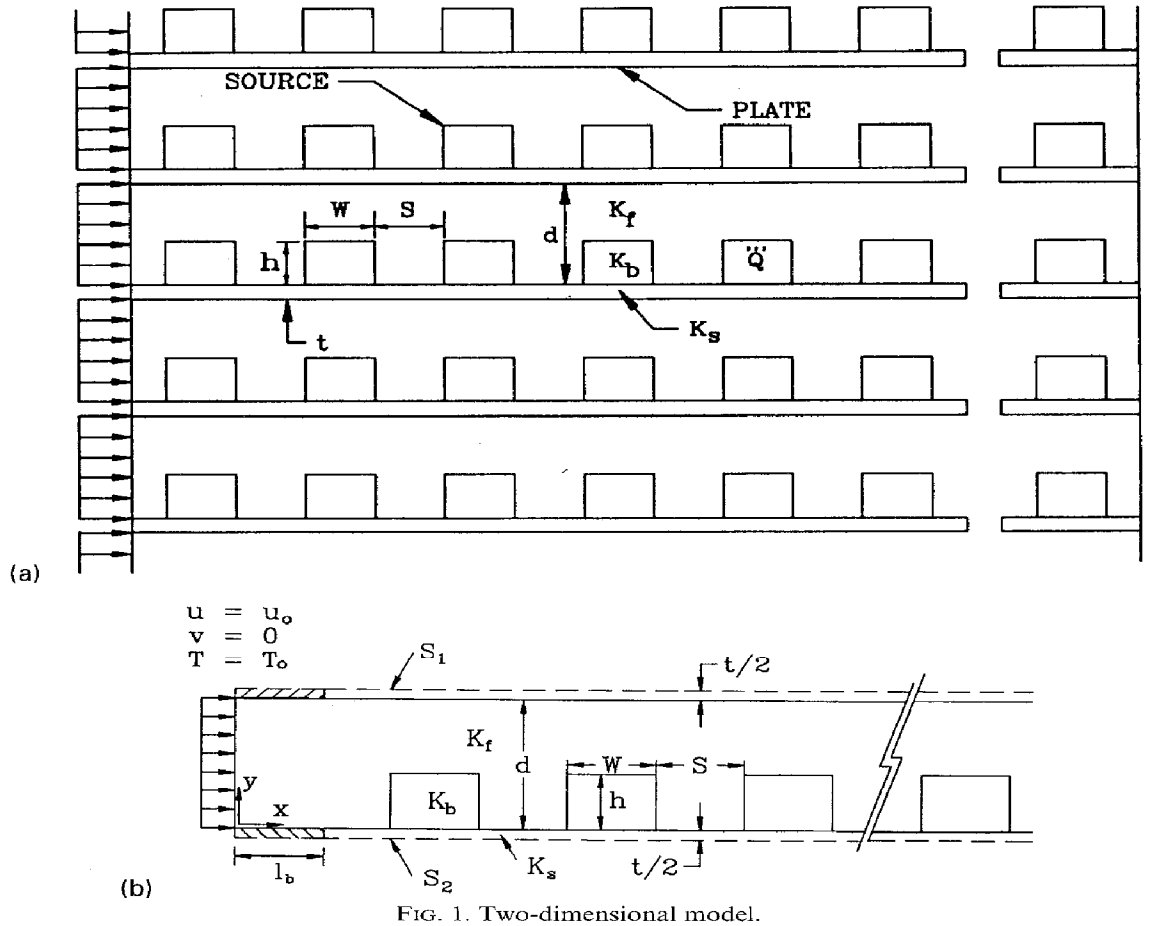

FIG. 1. Two-dimensional model.

the temperature field. Based on this discussion, the governing equations can be written as:

Continuity:

$$\frac{\partial u}{\partial x}+\frac{\partial v}{\partial y}=0, \tag{1}$$

X-momentum:

$$\rho\left(u\frac{\partial u}{\partial x}+v\frac{\partial u}{\partial y}\right)=-\frac{\partial p}{\partial x}+\frac{\partial}{\partial x}\left(\mu\frac{\partial u}{\partial x}\right)+\frac{\partial}{\partial y}\left(\mu\frac{\partial u}{\partial y}\right), \tag{2}$$

Y-momentum:

$$\rho\left(u\frac{\partial v}{\partial x}+v\frac{\partial v}{\partial y}\right)=-\frac{\partial p}{\partial y}+\frac{\partial}{\partial x}\left(\mu\frac{\partial v}{\partial x}\right)+\frac{\partial}{\partial y}\left(\mu\frac{\partial v}{\partial y}\right), \tag{3}$$

Energy:

$$\rho\left(u\frac{\partial T}{\partial x}+v\frac{\partial T}{\partial y}\right)=\frac{\partial}{\partial x}\left(K\frac{\mu}{Pr}\frac{\partial T}{\partial x}\right)+\frac{\partial}{\partial y}\left(K\frac{\mu}{Pr}\frac{\partial T}{\partial y}\right)+\frac{Q'''}{C_p}\delta, \tag{4}$$

where K is the ratio of the conductivity of the solid to the fluid (air) and δ is the Kronecker delta. The energy equation (4) governs temperature distribution in both fluid and solid regions. However, one needs to assign the appropriate conductivity (K) and δ so that:

Flow region: $K = 1$ $\delta = 0$, (5)

Block: $K = K_b/K_f$ $\delta = 1$, (6)

Substrate: $K = K_s/K_f$ $\delta = 0$, (7)

Interface: $K = K_i/K_f$ $\delta = 0$. (8)

The interface conductivity K_i obtained by the harmonic mean method as:

$$K_i = \frac{K_s K_f (Y_p + Y_s)}{K_s Y_p + K_f Y_s}, \tag{9}$$

where Y_p is the distance between the interface and the first node in the fluid region from the interface and Y_s is the distance between the interface and the first node inside the solid. When the harmonic mean is considered between the fluid and the block, K_b replaces K_s in the above equation. The harmonic mean in the streamwise direction should be replaced with X_p and X_s instead of Y_p and Y_s.

Boundary conditions for velocity and temperature fields need to be specified to solve the governing equations (1)–(4). Fluid is assumed to enter the channel with a uniform velocity and temperature profile, i.e. $x = 0$, $u = u_0$, $v = 0$, and $T = T_0$. It should be noted that an arbitrary location can be chosen for imposing

these inlet conditions. Imposing inlet conditions close to the first block results in a large deflection of stream lines which lead to a greater vena contracta effect and thus warrants a greater number of blocks so that the entry region can be free. A way to reduce this effect is to allow an inlet buffer length between the inlet and the first block. The length between the inlet and the first module is set to $l_b/w = 4$ for calculation purposes. Conduction in the substrate through the inlet buffer length is neglected by subjecting it to the adiabatic condition. A repeated boundary condition [13] is imposed at surfaces S_1 and S_2 (Fig. 1b) for the temperature field to simulate thermal coupling between two adjacent channels:
i.e.

$$K_s \frac{\partial T}{\partial y}\bigg|_{(x,-t/2)} = K_s \frac{\partial T}{\partial y}\bigg|_{(x,d+t/2)}$$

and

$$T_{(x,-t/2)} = T_{(x,d+t/2)}. \tag{10}$$

The substrate, in the stream-wise direction, is treated as insulated at the edges. The description of the governing equations and associated boundary conditions will be complete if the boundary condition for the fluid temperature at the channel outlet is specified. For this purpose an alternative (type-b) approach to the traditionally used natural condition (type-a) is proposed. A natural boundary treatment is not applicable at the outlet for the thermal field since a natural boundary condition represents local parabolicity and the fluid temperature field is not locally parabolic in the presence of wall conduction. The proposed type-b boundary condition is used at the channel exit to properly capture the elliptic effects. Because the blocks have heat sources of equal strength, the temperature difference between the centers of two successive blocks in the channel exit region is assumed to be same. The exit boundary is placed at the middle of the last block. The outlet condition for both fluid and solid (block and plates) temperature field can now be stated as:

$$\left(\frac{\partial T}{\partial x}\right)_{N-1} = \left(\frac{\partial T}{\partial x}\right)_N. \tag{11}$$

The above equation implies that the temperature rise between the center of the fourth and fifth block is the same as the temperature rise between the center of the fifth and sixth block. The natural boundary condition is applied at the exit for the flow field (type-b). No flow recirculation is expected at the exit because the exit boundary is placed at the middle of the last block. The superiority of the proposed boundary condition over the traditional natural condition is established by the authors and discussed in detail elsewhere [3, 18].

SOLUTION PROCEDURE

The governing equations are solved using a finite volume technique [19]. The velocity and pressure field are linked by the SIMPLER algorithm and a solution to a one-dimensional convection diffusion equation is represented by the power law. The focus of this paper is developing flow (*DF*) in channels. The discretization equations are solved by the line-by-line procedure, which is the combination of Gauss–Siedel and the Tri-Diagonal Matrix algorithm. The Cyclic Tri-Diagonal Matrix Algorithm (CTDMA) is used to solve a set of discretization equations along each line in the cross-stream direction while sweeping in the streamwise direction. The convergence criterion in this study is based on the relative value of the sums of the residuals of algebraic equations, as given below:

$$\frac{\sum |R_\phi|}{R_{\phi,\mathrm{ref}}} < 1 \times 10^{-5}, \tag{12}$$

where $\Sigma |R_\phi|$ is the sum of all absolute residuals over the entire flow field. The residuals are defined as:

$$R_\phi = a_p \phi_p - \sum a_{nb} \phi_{nb} - S. \tag{13}$$

In addition, successive changes in variables for the entire flow field are monitored and the following condition is used to declare convergence, i.e.

$$\mathrm{MAX}\left(\left|\frac{\phi_{I,J}^{K+1} - \phi_{I,J}^{K}}{\phi_{I,J}^{K+1}}\right|\right) \leqslant 1 \times 10^{-5}. \tag{14}$$

Convergence is declared if the above two conditions, equations (12) and (14), are satisfied. The focus of this work is developing flow (*DF*). However, the flow and heat transfer will be periodically fully developed (*PDF*), far from the channel entrance, if blocks are positioned in a periodic manner [12]. The flow and temperature field obtained as a solution to the *DF* problem should agree with the *PDF* problem solution far from the channel entrance. In fact, this criteria validates the proposed boundary condition (type-b). Details of the *PDF* problem and its solution procedure can be found in Kim [3, 18] and will not be discussed in this paper.

A grid independence study was performed by examining the impact of grid size on friction factor for modules and average Nusselt number for blocks. A module is a portion of a channel that includes one block and a length equal to the half-block spacing on either side of the block. Selection of the grid size for the *DF* problem is guided by the grid size for *PDF* problems. The number of control volumes for the *DF* problem, in the cross-stream direction, is the same as that for the *PDF* problem. The total number of grid lines in the streamwise direction is obtained by multiplying the number of control volumes in a *PDF* module by the number of blocks considered. The inlet buffer length is included in the computational domain for the developing flow problem. The resulting non-uniformly spaced grid sizes examined for the *DF* problem are 98×18, 153×26, 197×36, and 274×46.

Table 1. The effect of grid size on friction factor and average Nusselt number in developing flow ($Re = 2000$)

Module	No. of C.V.	f	$\overline{Nu_0}$
1	98 × 18	0.45931	7.421
	153 × 26	0.3969	6.872
	197 × 36	0.295	6.384
	274 × 46	0.2721	5.996
2	98 × 18	0.31642	5.546
	153 × 26	0.26366	5.609
	197 × 36	0.263	5.286
	274 × 46	0.2608	5.224
3	98 × 18	0.28265	4.804
	153 × 26	0.26324	4.785
	197 × 36	0.26122	4.611
	274 × 46	0.26213	4.563
4	98 × 18	0.23894	4.3
	153 × 26	0.24358	4.283
	197 × 36	0.2433	4.149
	274 × 46	0.24498	4.111
5	98 × 18	0.21119	3.956
	153 × 26	0.21503	3.954
	197 × 36	0.21611	3.839
	274 × 46	0.21962	3.804

Table 1 shows the friction factor and average Nusselt number for the *DF* problem for the case of maximum Reynold's number ($Re = 2000$) considered in this study. Friction factor per module is the average pressure drop per one module length and is defined as:

$$f = \frac{\bar{p}(x,y) - \bar{p}(x+l,y)}{l} \frac{2d}{(\rho u_b^2)/2}, \quad (15)$$

where:

$$\bar{p} = \frac{1}{d}\int_0^d p \, dy.$$

The average Nusselt number per block is given by:

$$\overline{Nu_0} = \frac{1}{(1+2h/w)} \int_0^{1+(2h/w)} Nu_0 \, d(z/w) \quad (16)$$

Nu_0 in the above equation is the Nusselt number based on the inlet temperature, i.e.:

$$Nu_0 = \frac{hw}{k_f} = \frac{q}{\theta_w - \theta_0}. \quad (17)$$

The variation in friction factor and the average Nusselt number was less than 2% between the grid sizes of 197 × 36 and 274 × 46 with the exception of the first module. The difference in the first module is due to the large deflection of streamlines because of an abrupt decrease in the flow area. The maximum error for the first module is 7% for the friction factor and 6% for the average Nusselt number. It is evident that the results of the 197 × 36 grid are reasonable when compared to those of the 274 × 46 grid. Therefore, the 197 × 36 non-uniform grid size is used for laminar developing flow. Typical grid distributions can be found in Kim [3]. In addition, the solution technique was validated by comparing numerically predicted Nusselt number with analytical solutions for flow and heat transfer between parallel plates [20, 21]. The comparison was extremely good and can be found elsewhere [3].

INDEPENDENT PARAMETERS

Examination of the governing equations reveals that the independent parameters are the Reynolds number (Re), Prandtl number (Pr), conductivity ratio of the solid to fluid (K_b/K_f and K_s/K_f), and geometrical parameters. The selection of the parametric range is guided by the actual values used in cooling the electronic components. Table 2 shows the parametric range adopted for this study. Typical fluids used are air, water and FC series liquids. In this study, air ($K_f = 0.025$ W m^{-1} °C^{-1}) is selected for its generality as a cooling fluid. The substrate is composed of a combination of an epoxy-glass, copper, or ceramic laminate. The effective conductivity has a range of 0.2–0.6 W m^{-1} °C^{-1} [2, 10]. However, the effective conductivity of the substrate has a range of thermal conductivity values due to varying amounts of material, i.e. copper alloy, silicon and soldering Beryllia [8, 10]. Beryllia is especially promising, in spite of manufacturing difficulties, and has a very high conductivity [17]. Therefore, values of the substrate conductivity between zero and a high value ($K_s/K_f = 20$) were chosen. For electronic packages, its effective conductivity is generally higher when compared to air because of the high conductivities of electronic component materials. A very high ratio of block conductivity to air ($K_b/K_f = 500$) is used to focus on the substrate effect. The geometrical parameters are the ratios of block height to block width (h/w), of block spacing to block width (s/w), and of channel height to channel width (d/w).

RESULTS AND DISCUSSION

The results presented in this section focus on the developing flow. However, the corresponding results for the *PDF* analysis are given for the purpose of comparison. No specific explanation for *PDF* is given in this paper, but, a detailed procedure of PDF analysis is presented in ref. [3]. Phrases such as "top surface" and "bottom surface" are defined here for the

Table 2. Range of independent parameters

Parameters	Range
Re	100, 500, 1000, 2000
Pr	0.7
K_b/K_f	500
K_s/K_f	0, 0.1, 1.0, 20
h/w	0.25, 0.5
s/w	0.25, 0.5, 1
$(d-h)/w$	0.25, 0.5, 1

purpose of clarity. The bottom surface includes the bottom wall surface of the channel and the surface of the block in contact with the fluid. The top surface refers to the top wall surface of the channel.

Flow field

The transverse velocity profiles in the streamwise direction are examined and compared with the periodically fully developed profiles. Figure 2 shows the transverse velocity profiles for the middle of the cavity (denoted by 'C') and the middle of the block (denoted by 'B') at the modules (denoted by numbers) in the streamwise direction. These profiles are also compared with the transverse velocity *PDF* profile. The velocities in these figures are normalized with the inlet velocity (u_o), which is the same as the bulk velocity (u_o). The transverse velocity profiles at the low Reynolds number ($Re = 100$) are shown to be coincident, starting downstream of the second module. These are also identical with the transverse velocity profiles for *PDF*. This implies that the flow is considered to have reached the periodically fully developed condition beginning from the second module. As the Reynolds number increases to a value of 1000, it can be seen that the velocity profiles are different from those for *PDF*. The flow field is shown to be developing further downstream and getting close to the *PDF* profiles. This is more pronounced as the Reynolds number is increased beyond 1000, and the profiles are farther from those for *PDF*. This is expected since a longer length or more modules in the entry region are required for the flow to reach the fully developed condition as the Reynolds number increases. Initially, the velocity profiles are skewed towards the top surface. This skewness decreases downstream of the first module. The maximum points of the profiles moves toward the center line of the flow path $(d-h)/2$, where the maximum point for the fully developed profile occurs. The velocity profile at the last module is now very close to that of the fully developed *PDF*

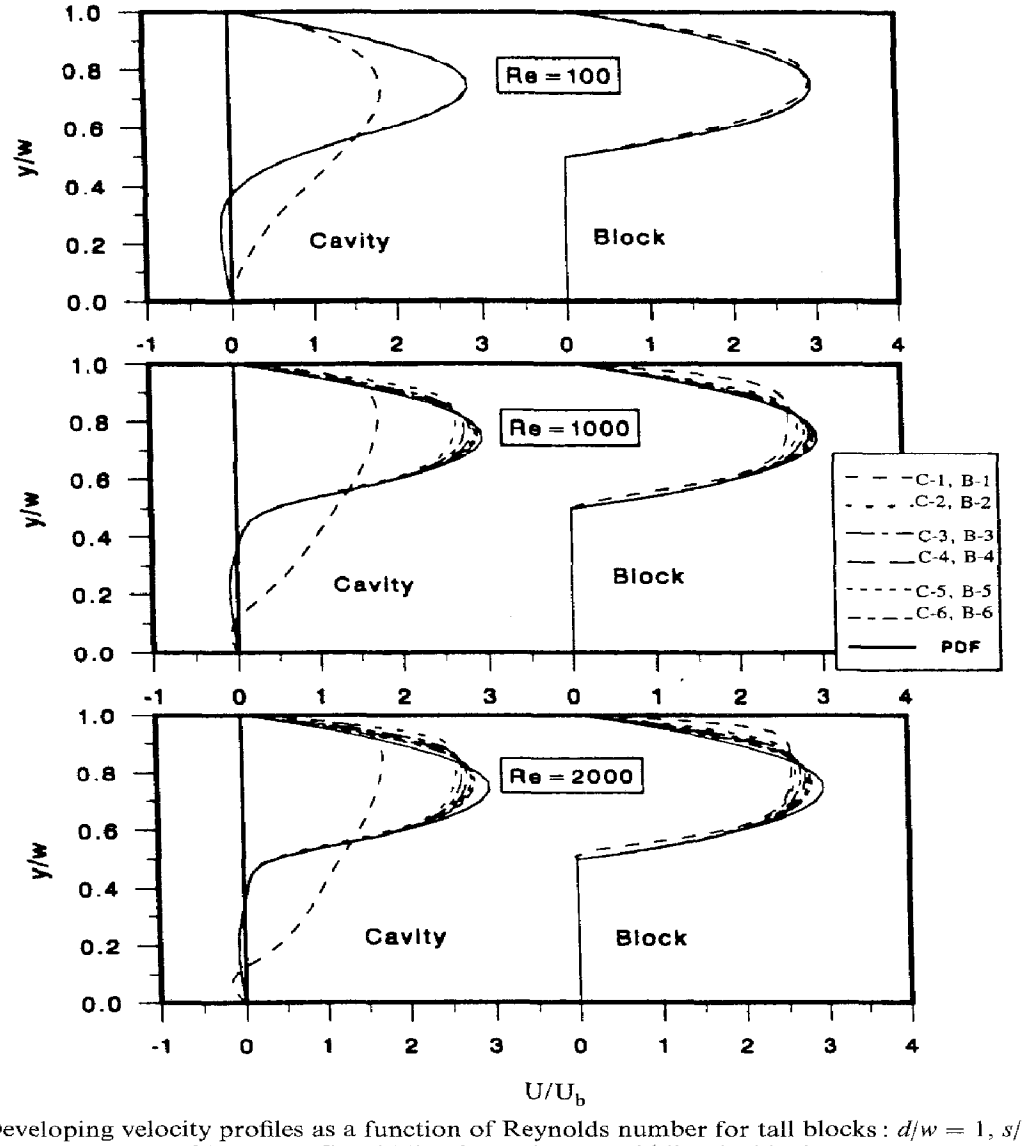

FIG. 2. Developing velocity profiles as a function of Reynolds number for tall blocks: $d/w = 1$, $s/w = 0.5$, $h/w = 0.5$, C: middle of a cavity, B: middle of a block.

profile. The above mentioned trends are the same for the channel with flat blocks and are reported elsewhere [3].

Figure 3 shows the developing velocity profiles for different block spacings (Fig. 3a) and channel heights (Fig. 3b). Only the velocity profiles at the middle of the cavity are presented since the qualitative variations of these profiles at the middle of the cavity and block are similar. The channel with a larger block spacing, for the same cross-sectional area of flow and Reynolds number seems to reach the fully developed condition with a fewer number of modules. Note that the channel with a larger block spacing represents a longer length in the streamwise direction. The recirculation flow in the cavity for a smaller block spacing is very weak and, furthermore, the fluid has nearly no motion at the bottom half of the cavity. As the block spacing increases, the magnitude of the recirculation flow is shown to increase and penetrate up to the bottom half of the cavity.

For a smaller channel height (see Fig. 3b), the flow reaches the fully developed condition with a fewer number of modules. Note that the growth of the boundary layer (thickness) depends only on the Reynolds number. For this reason the boundary layers (from the top and bottom surfaces) meet in a shorter distance from the inlet for the channel with smaller heights. As the channel height is reduced, the presence of the block is felt by the fluid flow so the strength of the recirculation flow in terms of the magnitudes of the negative velocities in the cavity becomes more active. However, the nature of the velocity profiles in the streamwise direction is similar but the magnitudes become progressively weak as the channel height increases.

The friction factor for DF is examined with respect to different parameters considered in this study. This friction factor is also compared with those for PDF, which is shown as symbols on the right side of each figure. The friction factor for developing channel flow

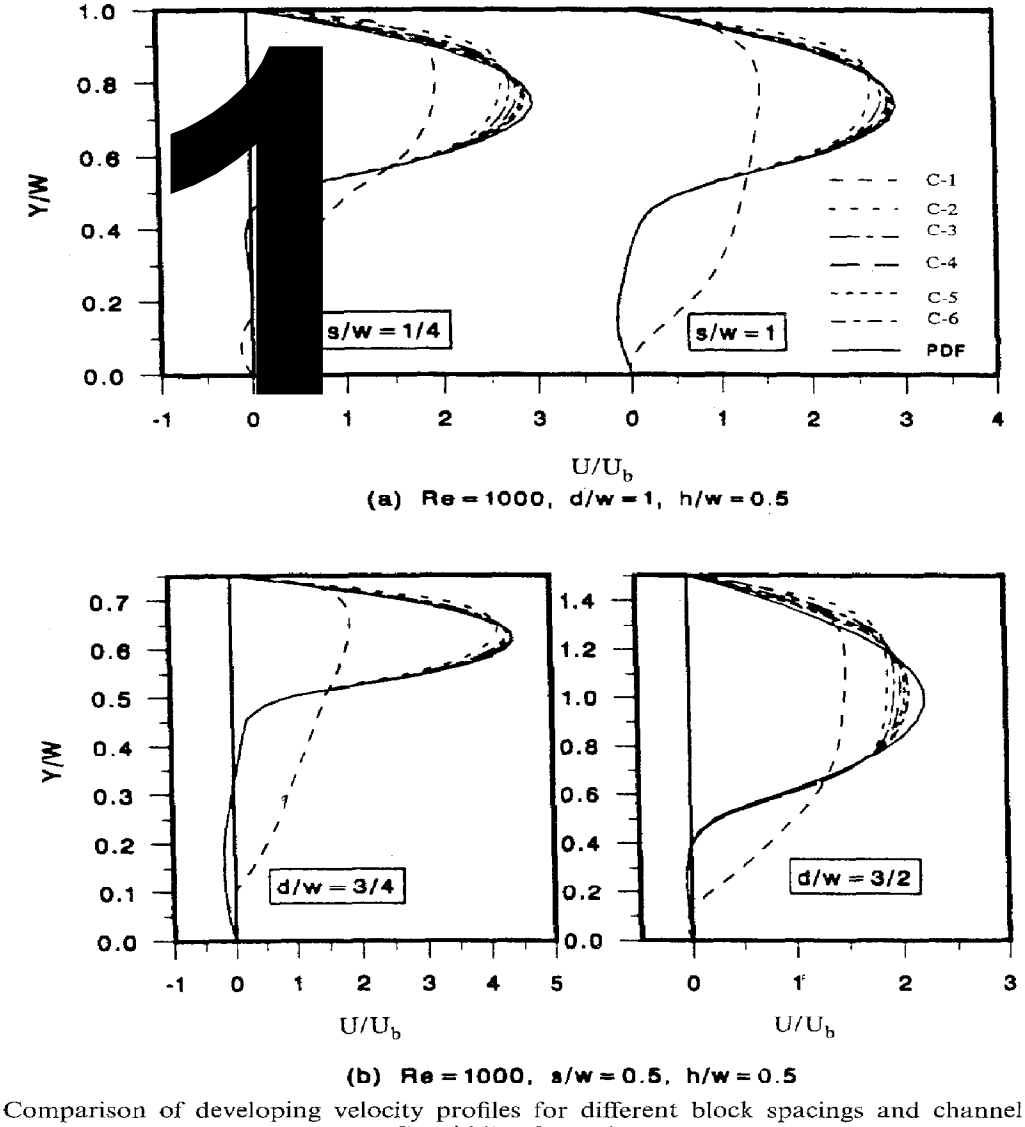

FIG. 3. Comparison of developing velocity profiles for different block spacings and channel heights: C: middle of a cavity.

is defined as average pressure drop per module length as in equation (15). The definition of friction factor, based on the smooth channel, enables a direct comparison between the smooth channel and the channel with blocks.

Figure 4 shows the variation of friction factor for modules in the streamwise direction and the corresponding friction factor for *PDF* for tall blocks. In general, the friction factor gradually decreases in the streamwise direction after a large drop at the first module. The friction factors for *DF* approach those of *PDF*, which implies that flow is reaching the periodically fully developed condition in the streamwise direction. It can be inferred that, for some cases, the friction factor for *DF* at the outlet can be close to the values for *PDF*. These cases show that the flow has reached the periodically fully developed condition. In other cases, where the values are not close enough, the flow has not yet reached the periodically fully developed condition. Evidently, the entry length is shortened for the lower value of the Reynolds number (Re), channel height (d/w), and the larger value of block spacing. It can be seen that the friction factor strongly depends on the channel height and weakly depends on the block spacing. This is plausible since, from a physical point of view, the friction factor for a channel with the larger block spacing should be closer to that of a parallel plate channel ($f = 0.96$). The friction factors, for the lower Reynolds number, maintain almost constant values downstream of the second module. These values are shown to be the same value as those for *PDF*. The absolute values of the friction factors are reduced as the Reynolds number increases, although the trends remain the same. As shown, the friction factors for *DF* with different block spacings converge slightly farther downstream so the effect of block spacing is diminishing. It is apparent that the effect of block spacing is minimal on the friction factors for *PDF*. However, the effect of channel height remains almost the same. At high Reynolds numbers and large values of the channel height, the friction factors in the second module happen to be less when compared to those for the downstream modules. This is because of the recirculation pocket occurring at the top of the first block that affects the pressure field. It should be noted that the average pressure is employed for estimating the friction factor in the present study. Generally, the trends for the tall blocks remain the same as for flat blocks, although the values are smaller for the flat blocks [3].

Thermal field

For the purpose of studying the temperature field, a non-dimensional temperature (θ) is defined as:

$$\theta = \frac{(T - T_0)}{Q''' wh/K_f}. \tag{18}$$

As seen in equation (18), the inlet temperature is no longer available for the *PDF* module because a module is isolated for the computational domain. There should be a provision for directly comparing the thermal field between *DF* and *PDF* because the current practice does not provide a common ground for comparison. Hence, there is a need to define a reference temperature other than the inlet tempera-

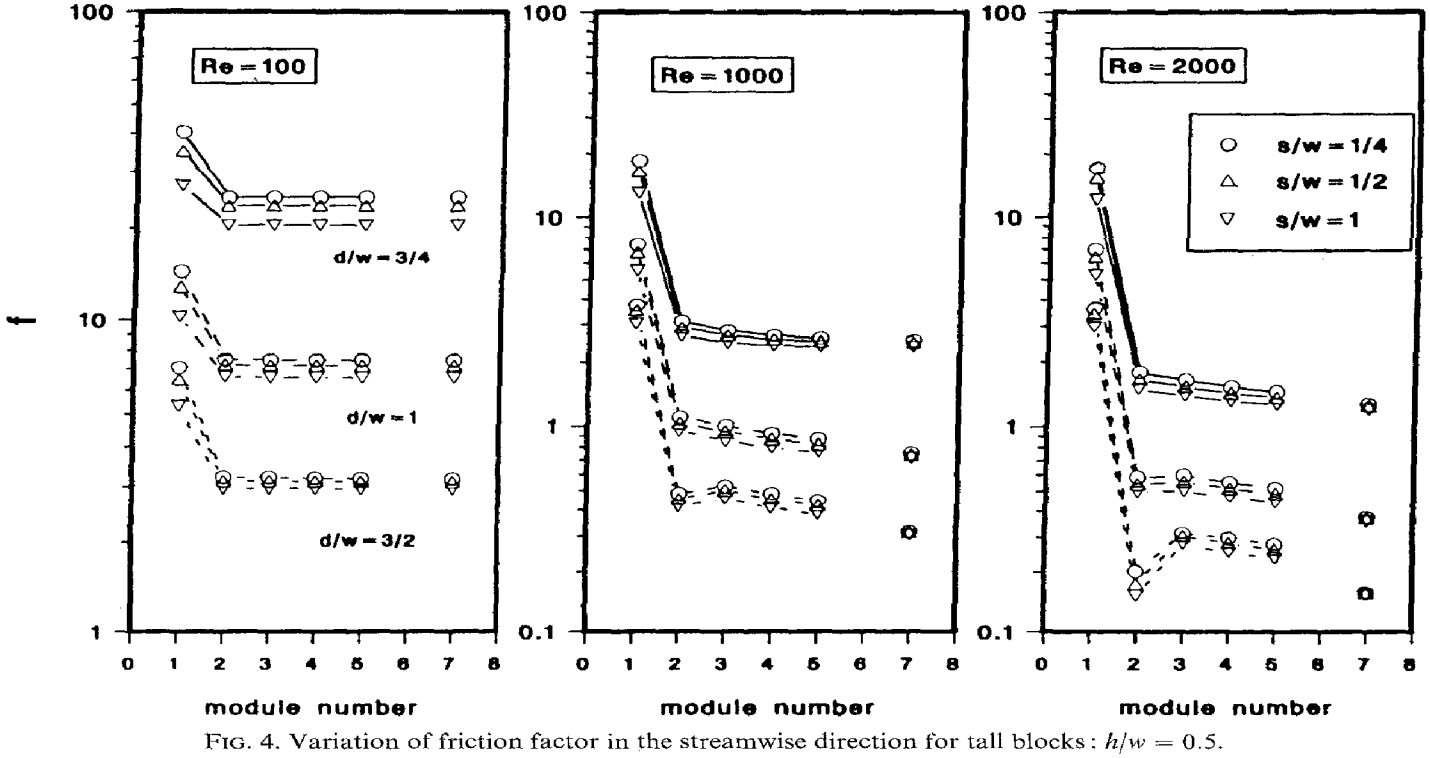

FIG. 4. Variation of friction factor in the streamwise direction for tall blocks: $h/w = 0.5$.

ture. Moffat *et al.* [7] originally proposed the concept of the adiabatic temperature as a reference temperature to eliminate the thermal wake effects from the upstream heating. This concept was derived from the fact that temperatures after the first four or five modules simply increase due to an increase in the bulk temperature. In mathematical form, the temperature difference between any location and the inlet can be defined as:

$$(\theta-\theta_0) = (\theta-\theta_{ref})+(\theta_{ref}-\theta_0), \quad (19)$$

where θ_{ref} is a reference temperature.

Moffat *et al.* [7] defined the adiabatic temperature as the reference temperature obtained from the superposition of the Kernel function, i.e. the temperature rise on a module due to heating by the upstream modules on the mean temperature rise. The definition of the adiabatic temperature can be used independently of the flow and heating condition. However, the information at the inlet should be given in order to get the adiabatic temperature.

A simple alternative for the aforementioned difficulties is to use the bulk temperature (θ_b) upstream of the modules as a reference temperature (θ_{ref}). The bulk temperature can be easily obtained for both *DF* in channels and *PDF* in modules. In this study, only a constant heat source is considered so the bulk temperature is free from the effect of different upstream heating conditions. To account for the recirculation flow [22, 23], the bulk temperature is defined as:

$$\theta_b = \frac{\int_0^{d/w} |u|\,\theta\,dy}{\int_0^{d/w} |u|\,dy}. \quad (20)$$

The non-dimensional temperature difference $(\theta-\theta_b)$ can be defined with the bulk temperatures upstream of each *DF* channel module and enables comparison of the temperature field directly for *DF* and *PDF*. For convenience, let the module temperature of *DF* be defined as:

$$\theta_m = \theta-\theta_b. \quad (21)$$

The module temperature (θ_m) represents the temperature rise by self-heating within a module that removes the thermal wake effects from the upstream heating.

Figure 5 shows the isotherms in terms of module temperature (θ_m). The isothermal lines for each module now remove the thermal wake effect due to upstream heating. At the low Reynolds number ($Re = 100$), the isothermal lines of θ_m apparently have a different shape from the isothermal lines of θ [3]. The distribution patterns of each module are similar to each other starting from the second module. At the high Reynolds number ($Re = 2000$), the isothermal lines of θ_m are shown to be not much different than those of θ [3]. In this case, the increase of the bulk temperature is small because the Reynolds number is high. It is apparent that θ_m is still increasing in the downstream direction. The same qualitative results can be obtained when the substrate conduction is considered for both low and high Reynolds numbers [3].

Temperature distribution

Figure 6 shows the module temperature variations along the top and bottom surfaces. The module temperature distributions for the *PDF* analysis are presented at the right-hand side of each figure. At low Reynolds number ($Re = 100$) the module temperature is nearly constant downstream of the second module and is same as for the *PDF* both in magnitude and shape. At higher Reynolds number ($Re \geqslant 1000$) the module temperatures continue to vary along both top and bottom surfaces, and they have yet to reach those for *PDF*. This implies that the thermal field is fully developed starting from the second module at $Re = 100$ but is still in the developing stage for $Re \geqslant 1000$. The difference between the module temperature for *DF* and *PDF* is the indicator in deciding whether the flow is thermally developing or periodically fully developed. A negative temperature along the top surface implies that the actual surface temperature is less than the bulk temperature. The trends of module temperature distribution with substrate conduction (Fig. 6b) are similar to the adiabatic case. In the presence of wall conduction the module temperatures for *DF* and *PDF* are closer, implying that the wall conduction reduces the thermal entry length. It is because the conducting substrate aids thermal energy transfer to the top surface that thermal boundary layers grow at the top of the block and on the top surface as well. Thermal boundary layers from both these surfaces share the dissipation of thermal energy to the main bypass flow so the temperature fields attain a periodically fully developed condition in a shorter distance from the inlet.

Figure 7 shows the module temperature distributions in the transverse direction at the middle of the blocks. These are also compared with the module temperature distributions for *PDF*. A positive value for θ_m represents a higher temperature than the bulk temperature and vice versa. The temperature distributions at different locations (see legend) are such that a high temperature exists near the block and decreases in the transverse direction. Depending on K_s/K_f, the temperature distribution is different near both the bottom and top surfaces. As expected when an adiabatic substrate is considered, the minimum temperatures are located near the top surface. Note that the temperatures in the transverse direction monotonically decrease.

As the value of the conductivity increases to a value of 0.1, the temperature near the top surface sharply turns to positive values, and implies that some heat is being transferred through the substrate which, in turn, reduces the block temperature. The point of the minimum temperature shifts downwards because of diffusion in the fluid at the top surface. It should be

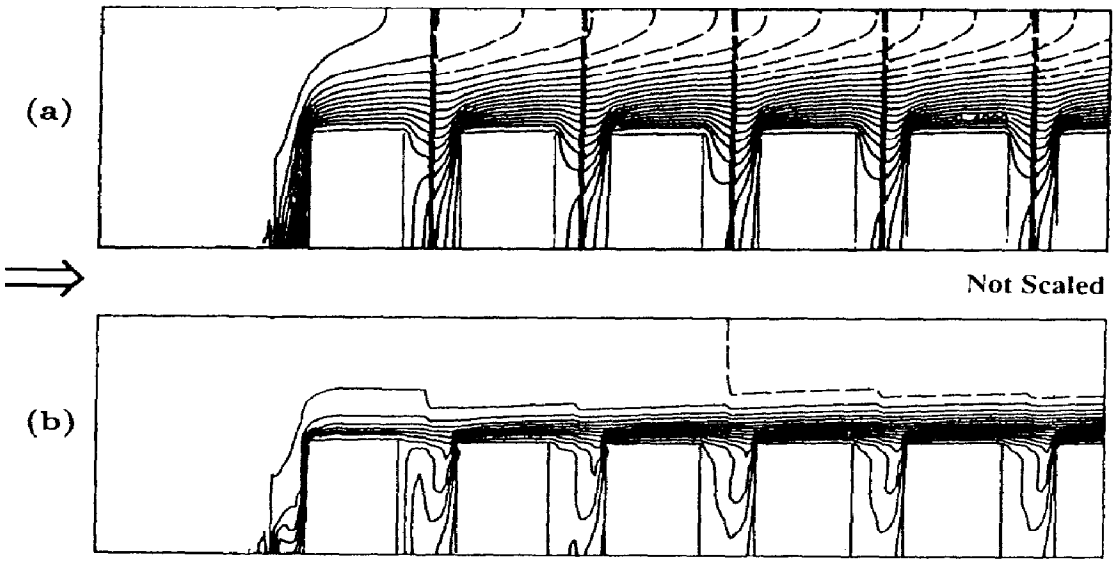

FIG. 5. Typical isotherm in terms of θ_m with an adiabatic substrate: $K_s/K_f = 0$, $d/w = 1$, $h/w = 0.5$, $s/w = 0.5$: (a) $Re = 100$, $\theta_m = -0.05$–0.16; (b) $Re = 2000$, $\theta_m = -0.01$–0.08.

noted that the locus of the minimum temperature in the streamwise direction is moving towards the top surface. The temperatures at the bottom surface are reduced further if the conductivity is higher ($K_s/K_f = 1$). The minimum temperature is shifted towards the center of the main bypass flow region, $(d-h)/2$, and its locus is coincident with the center line of the main bypass region. However, careful observation of the figure reveals that the locus of the minimum temperature has moved away from the top surface in the downstream direction and approaches that of *PDF*. This is due to the axial conduction in the substrate so that heat flows from the outlet towards the inlet and is released through the top surface to the fluid. The same trend is found in the temperature distribution if conductivity is increased further ($K_s/K_f = 20$). Temperatures at the blocks are reduced and the same behavior of the points of the minimum temperatures is found in the streamwise direction. The temperatures at the top and bottom surfaces reach almost the same value for $K_s/K_f = 20$. It should be noted that the behavior of the locus of the minimum temperature in the streamwise direction is very important to verify the repeated boundary condition in the transverse direction. The repeated condition was obtained in the work of Davalath and Bayazitoglu

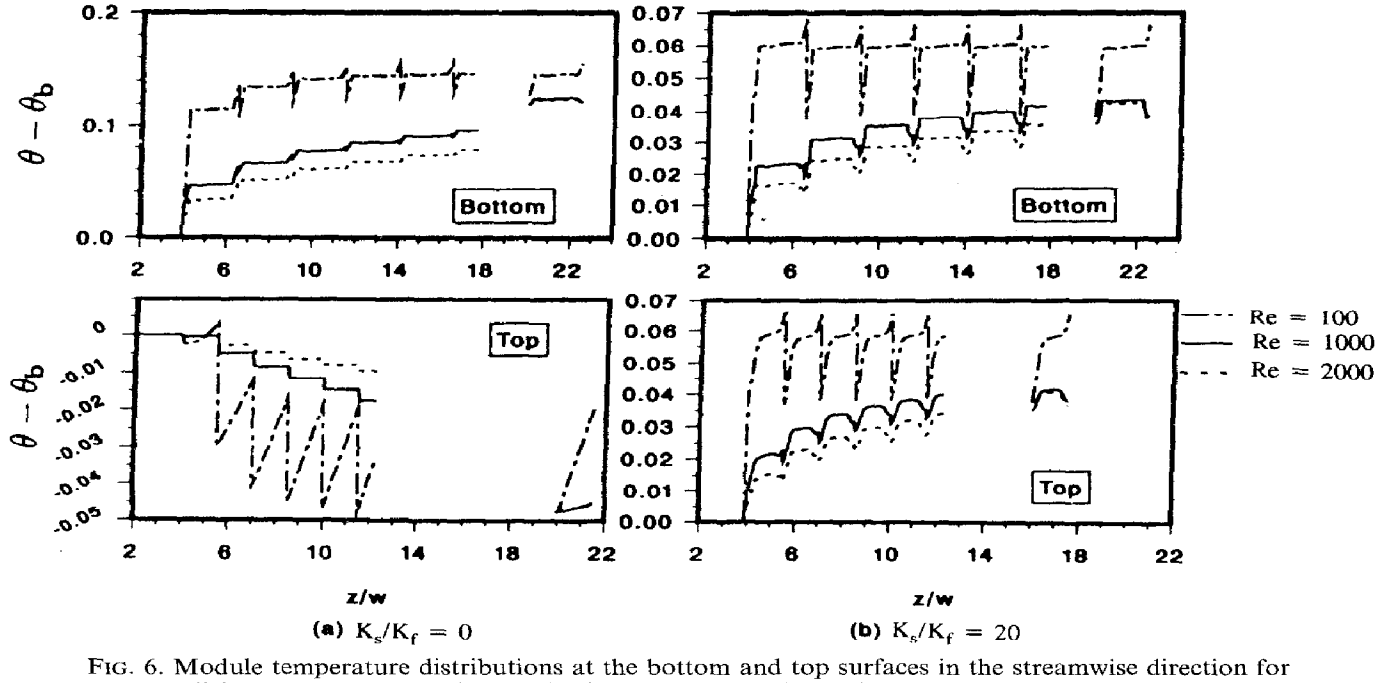

FIG. 6. Module temperature distributions at the bottom and top surfaces in the streamwise direction for different Reynolds numbers and substrate conductivities: $d/w = 1$, $h/w = 0.5$, $s/w = 0.5$.

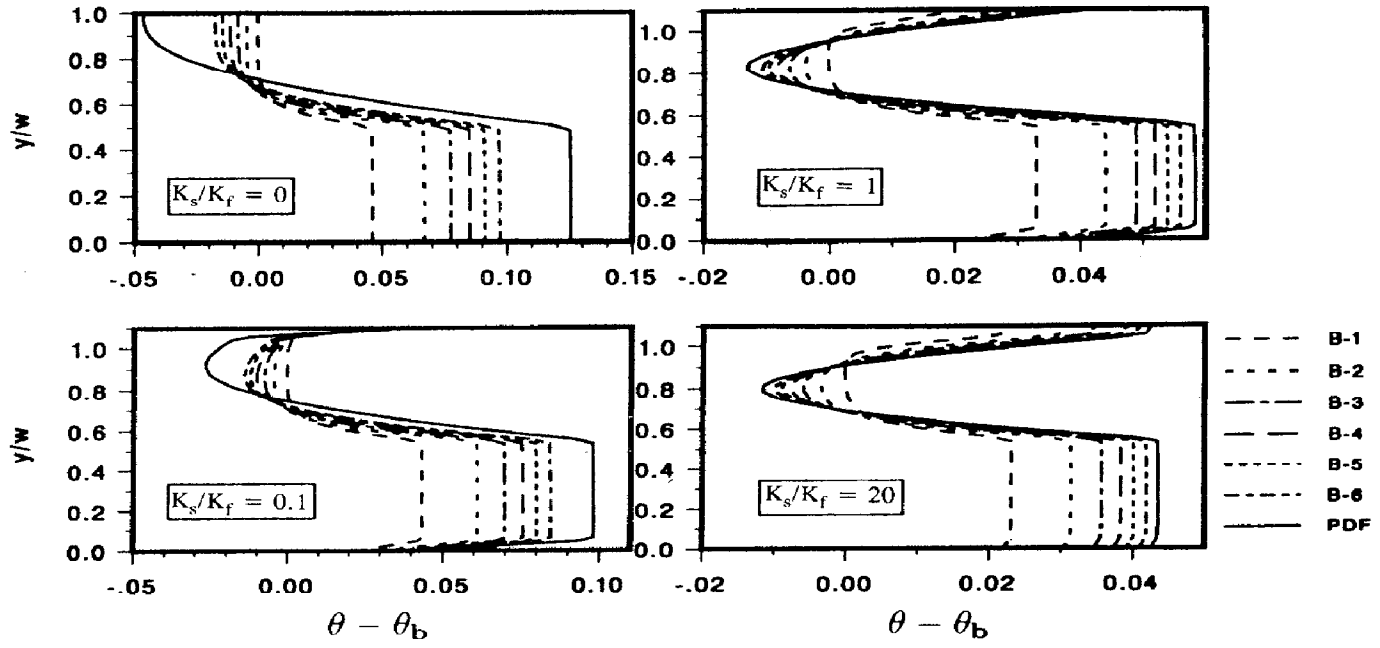

FIG. 7. Distributions of θ_m in the transverse direction for different substrate conductivities: $Re = 1000$, $d/w = 1$, $h/w = 0.5$, $s/w = 0.5$, B: middle of a block.

[16] by imposing a zero temperature gradient at the maximum velocity location in the transverse direction. However, as seen in the developing flow, the locus of the maximum velocity is not coincident to that of the minimum temperature in the streamwise direction and, furthermore, the locus of the minimum temperature is more likely to be controlled by conduction, so they are not in the same line (distance from the top surface).

Thermal resistance

The thermal performance of a heat sink in an electronic cooling area is often specified in terms of its overall resistance. Only the average and local Nusselt number distributions are indicators of the thermal performance of blocks whose heat dissipation path is through the cooling fluid. However, heat transfer in cooling channels of electronic components comprises convective cooling, conduction cooling, and/or both cooling modes. Hence, thermal resistance is a better indicator to measure the cooling performance. It should be noted that the resistance in convective cooling is the reciprocal of the Nusselt number. Nevertheless, local and average Nusselt number distributions were studied in detail [3] but not presented in this paper due to space restrictions. Thermal resistance per unit length in this study is defined as the temperature difference between the maximum temperature inside the block and the reference temperature to the total heat generated by the heat source, i.e.:

$$R_t = \frac{(T_{max} - T_{ref})}{Q''' wh}. \quad (22)$$

The non-dimensional form of the thermal resistance is:

$$\bar{R} = R_t K_f = (\theta_{max} - \theta_{ref}). \quad (23)$$

The non-dimensional thermal resistance physically represents the difference between the maximum and reference temperatures for each module. The resistance is defined with the channel inlet temperature or the module inlet bulk temperature as $\bar{R}_0$ and $\bar{R}_m$, respectively. The relation between $\bar{R}_0$ and $\bar{R}_m$ becomes simply as follows:

$$\bar{R}_0 = \bar{R}_m + (\theta_b - \theta_0). \quad (24)$$

Figure 8 shows the distributions of $\bar{R}_0$ and $\bar{R}_m$ in the streamwise direction for different Reynolds numbers and substrate conductivities. The corresponding $\bar{R}_m$ for *PDF* is also presented for comparison purposes at the right side of each plot. For the distribution of $\bar{R}_0$ at the Reynolds number of 100, the thermal resistance increases in the streamwise direction. The entry effect can be seen at the first module for the adiabatic case so the gradient between the first and second modules is higher for any two adjacent modules.

Except for the above case, the gradient downstream from the second module increases quite linearly. It is clear that if the substrate conductivity increases the thermal resistance decreases and its gradient in the streamwise direction becomes nearly constant, which can be interpreted as approaching the periodically fully developed flow. The distribution of R_0 is directly reflected in the distribution of $\bar{R}_m$. Since the effect of the upstream heating is removed, the values of $\bar{R}_m$ are less than those of $\bar{R}_0$. It can be easily seen if the thermal

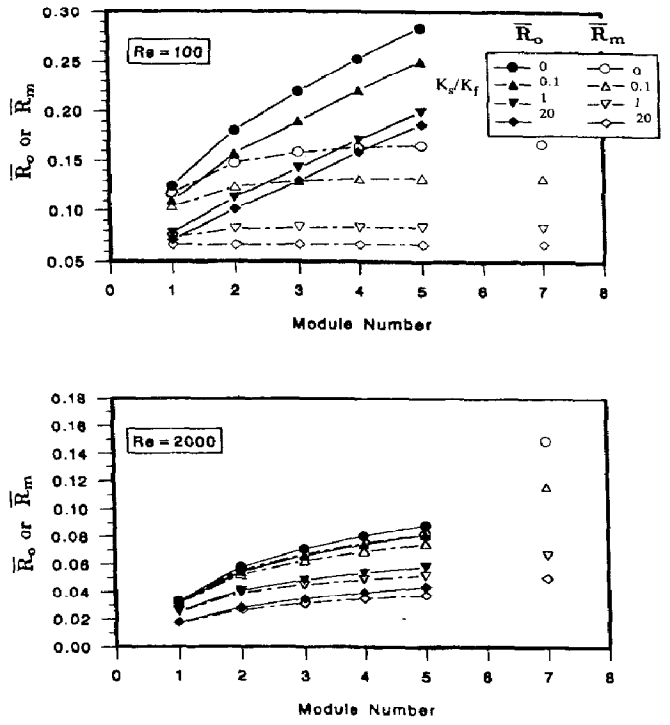

FIG. 8. Variation of thermal resistance in terms of $\bar{R}_0$ and $\bar{R}_m$ in the streamwise direction with respect to Reynolds number and substrate conductivity: $s/w = 0.5$, $d/w = 1$, $h/w = 0.5$.

field is periodically fully developed or not by comparing $\bar{R}_m$ for *DF* with $\bar{R}_m$ for *PDF*. As shown, $\bar{R}_m$ for *DF* increases slightly and maintains nearly the same value as $\bar{R}_m$ of *PDF*. As explained earlier, the thermal field attains the periodically fully developed condition within the first few modules if the substrate conductivity is higher. The effect of the substrate conductivity on either $\bar{R}_0$ or $\bar{R}_m$ is consistent with the substrate conduction reducing the thermal resistance. It is clear from this study that the use of the thermal resistance is more appropriate in evaluating the cooling performance in the combined cooling mode (convection and conduction). As Reynolds number increases, the thermal resistance decreases. The increasing trend in the thermal resistance in the streamwise direction in all the range of the substrate conductivity is observed. It should be noted that at the high Reynolds number ($Re = 2000$), the distributions of $\bar{R}_0$ in the streamwise direction is shown to increase almost linearly. This distribution is similar to the periodically fully developed condition. However, as seen in the distribution of $\bar{R}_m$, it is far from the fully developed flow. Consequently, one should not declare that the thermal field is periodically fully developed at high Reynolds number ($Re = 2000$) simply by comparing the thermal resistance between the neighboring modules.

The correlations of thermal resistance in developing laminar flow are obtained from the least squares method in terms of $\bar{R}_0$ and $\bar{R}_m$. Since the thermal resistance downstream from the fifth block is not available, no attempt is made to correlate the data from *DF* to match that for *PDF* but, instead, the individual module is correlated with the given parameters. To be consistent with the correlations for *PDF*, the independent variables are selected and correlations are:

$$\bar{R}_0 = a_1 Re^{a_2}\left(1-\frac{h}{d}\right)^{a_3}\left(1+\frac{s}{w}\right)^{a_4}\left(\frac{d}{w}\right)^{a_5}\left(\frac{t}{h}\right)^{a_6}\left(\frac{K_s}{K_f}\right)^{a_7}, \tag{25}$$

$$\bar{R}_m = b_1 Re^{b_2}\left(1-\frac{h}{d}\right)^{b_3}\left(1+\frac{s}{w}\right)^{b_4}\left(\frac{d}{w}\right)^{b_5}\left(\frac{t}{h}\right)^{b_6}\left(\frac{K_s}{K_f}\right)^{b_7}. \tag{26}$$

The constants for a and b are presented in Tables 3 and 4 along with their statistical data in terms of standard deviation (*SD*), standard error of estimation (*SEE*), and coefficients of determination (*COD*). The correlations are made for adiabatic and conducting substrates separately.

SUMMARY

Flow and thermal characteristics for the channel with surface mounted heat generating blocks are numerically studied for the developing laminar flow case. Identical channels are repeated in the transverse direction and each channel is thermally coupled with the neighboring channels via the finitely conducting substrate. A channel is isolated as a calculation domain by utilizing the repeated condition inside the substrate. The length of the channel is taken to be equal to that of five and a half modules. The results are also compared with those from the analysis of the periodically fully developed flow.

(1) By the nature of the channel configuration of electronic components, the use of the repeated condition in the transverse direction is essential when substrate conduction is included. The repeated boundary condition used in this study is found to be appropriate and also is confirmed with a series of natural convection channels where the velocity field is strongly dependent on the thermal field [12].

(2) The overall thermal resistance on a module by module basis is confirmed to be convenient and enables a direct comparison with those for *PDF* analysis. By defining the non-dimensional temperature based on the inlet bulk temperature in each module, the effect of self-heating of a module (removes the effect of upstream heating) can be analysed.

(3) As expected, the average module based thermal resistance for the blocks decreases with an increase in Reynolds number and increases in the streamwise direction. The substrate conduction appears to redistribute the heat flux by allowing part of the energy to the substrate, and in turn to

Table 3. Correlation constants for thermal resistance ($\bar{R}_0$) in developing flow and their statistical data

K_s/K_f	Constant	Module number 1	2	3	4	5
$K_s/K_f = 0$	a_1	1.269	1.757	2.237	2.716	3.213
	a_2	−0.415	−0.388	−0.394	−0.4037	−0.4149
	a_3	0.616	0.585	0.5773	0.5688	0.5586
	a_4	−0.0837	−0.309	−0.3614	−0.3823	−0.3931
	a_5	0.5042	0.5813	0.5778	0.5704	0.563
	SD	0.76	0.562	0.567	0.5755	0.584
	SEE	0.0312	0.0146	0.0237	0.364	0.0488
	COD	0.9972	0.9994	0.9984	0.9962	0.9935
$K_s/K_f > 0$	a_1	0.8599	1.212	1.7114	2.3084	2.9985
	a_2	−0.3978	−0.390	−0.4129	−0.4386	−0.4631
	a_3	0.5587	0.4955	0.4564	0.4216	0.3932
	a_4	−0.2056	−0.3204	−0.3504	−0.3611	−0.3655
	a_5	0.490	0.5178	0.520	0.5219	0.5235
	a_6	0.02824	0.0261	0.0424	0.05764	0.0706
	a_7	−0.1061	−0.1024	−0.0952	−0.08964	−0.08512
	SD	0.583	0.571	0.582	0.602	0.627
	SEE	0.0656	0.0706	0.0896	0.106	0.11
	COD	0.988	0.9854	0.9776	0.9710	0.966

the neighboring channel. This results in reduction of the temperature inside the block, which is very favorable in electronic component cooling. Even with a small conductivity ratio (K_s/K_f), the module thermal resistance is reduced, which highlights the importance of substrate conduction. When substrate conduction is included in the analysis, the thermal resistance seems to be a better indicator than the Nusselt number. Thermal resistance decreases with an increase in the Reynolds number, block spacing, and the substrate conductivity and increases with an increase in the area of bypass flow ($1-h/d$), substrate thickness (t/w), and height of the block (h/w). As a result of this study on thermal resistance, correlations for $\bar{R}_0$ and $\bar{R}_m$ in terms of independent parameters, are developed.

(4) As expected, the entry length based on the comparison between *DF* and *PDF* is reduced with a decrease in the Reynolds number and channel height and an increase in the block spacing. The thermal entry length is also found to be a function of the substrate conduction so that increase in the substrate conductivity results in decreasing the entry length. One should be careful to declare the number of modules in the streamwise direction where the thermal field is periodically fully developed. In laminar flow at high Reynolds numbers, it is shown that even a small difference of thermal resistance (Nusselt number) between the

Table 4. Correlation constants for module thermal resistance ($\bar{R}_m$) in developing flow and their statistical data

K_s/K_f	Constant	Module number 1	2	3	4	5
$K_s/K_f = 0$	b_1	1.22	1.162	1.105	1.038	0.9783
	b_2	−0.41	−0.325	−0.287	−0.259	−0.237
	b_3	0.6345	0.715	0.758	0.7874	0.809
	b_4	−0.043	−0.365	−0.453	−0.501	−0.535
	b_5	0.494	0.633	0.669	0.694	0.713
	SD	0.574	0.538	0.527	0.521	0.517
	SEE	0.0305	0.0371	0.0465	0.512	0.0536
	COD	0.9974	0.9955	0.9927	0.9910	0.990
$K_s/K_f > 0$	b_1	0.8132	0.5683	0.4990	0.4566	0.4290
	b_2	−0.3913	−0.285	−0.2410	−0.2130	−0.193
	b_3	0.5612	0.7263	0.7670	0.7920	0.8086
	b_4	−0.1654	−0.3653	−0.4410	−0.4851	−0.5171
	b_5	0.4876	0.530	0.5620	0.5876	0.6106
	b_6	0.0378	−0.0428	−0.0466	−0.0458	−0.0429
	b_7	−0.1077	−0.1186	−0.1202	−0.1214	−0.1224
	SD	0.5775	0.528	0.513	0.508	0.507
	SEE	0.0628	0.0561	0.0640	0.0703	0.076
	COD	0.9887	0.9892	0.9851	0.9820	0.9786

modules does not suggest the exact location of the periodically fully developed flow. It should be compared with the results of *PDF*. Therefore, the study of thermal characteristics in the periodically fully developed flow assumes a prominent place in this respects. Also, thermal characteristics of *PDF* can be used for a conservative basis of the electronic component cooling design.

Acknowledgements—The initial stages of the code development was supported by the Texas State Energy Research in Applications Program (ERAP, Contract # 32121-70340). The supercomputer time (CRAY-YMP) was made available through a grant from the Texas A&M University Supercomputer Center.

REFERENCES

1. W. Nakayama, Survey of design approaches in Japanese computer, International Symposium on Cooling Technology, Honolulu, U.S.A. (1987).
2. F. P. Incropera, Convection of heat transfer in electronic equipment cooling, *ASME J. Heat Transfer* **110,** 1097–1110 (1988).
3. S. H. Kim, A numerical analysis of convective heat transfer in channels simulating electronic components, Ph.D. Thesis, Texas A&M University (May 1993).
4. Y. Asako and M. Faghri, Three-dimensional heat transfer and fluid flow analysis of arrays of square blocks encountered in electronic equipment, *Numer. Heat Transfer* **13,** 481–498 (1988).
5. E. M. Sparrow, J. E. Niethammer and A. Chaboki, Heat transfer and pressure drop characteristics of array of rectangular modules encountered in electronic equipment, *Int. J. Heat Mass Transfer* **25,** 961–973 (1982).
6. G. L. Lehmann and R. A. Wirtz, The effect of variation in streamwise spacing and length on convection from surface mounted rectangular components, *Heat Transfer Electron. Equipment, ASME HTD* **48,** 39–47 (1985).
7. R. J. Moffat, D. E. Arvizu and A. Ortega, Cooling electronic components: forced convection experiments with an air cooled array, *Heat Transfer Electron. Equipment, ASME-HTD* **48,** 17–27 (1985).
8. S. Sridhar, M. Faghri, R. C. Lessmann and R. Schmidt, Heat transfer behavior including thermal wake effects in forced air cooling of arrays of rectangular blocks, *ASME HTD* **153,** 15–26 (1990).
9. R. A. Wirtz and W. Chen, Laminar-transitional convection from repeated ribs in a channel, *ASME-HTD* **171,** 89–94 (1991).
10. S. Sathe and Y. Joshi, Natural convection liquid cooling of a substrate mounted protrusion in a square enclosure: effect of thermophysical properties, geometric dimensions and boundary conditions, *Thermal Model. Des. Electron. Syst. Devices, ASME HTD* **153,** 73–80 (1990).
11. G. P. Peterson and A. Ortega, Thermal control of electronic equipment and devices, *Adv. Heat Transfer* **20,** 181–314 (1990).
12. S. H. Kim and N. K. Anand, Periodically fully developed flow in channels with conducting blockages, *AIAA J. Thermophys. Heat Transfer* **6,** 91–97 (1992).
13. S. H. Kim, N. K. Anand and L. S. Fletcher, Free convection between series of vertical parallel plates with embedded line heat source, *ASME J. Heat Transfer* **113,** 108–115 (1991).
14. S. Ramadhyani, D. F. Moffat and F. P. Incropera, Conjugate heat transfer from small isothermal heat sources embedded in a large substrate, *Int. J. Heat Mass Transfer* **28,** 1945–1952 (1985).
15. F. P. Incropera, J. S. Kerby, D. F. Moffat and S. Ramadhyani, Convection heat transfer from discrete heat sources in a rectangular channel, *Int. J. Heat Mass Transfer* **29,** 1052–1058 (1986).
16. J. Davalath and Y. Bayazitoglu, Forced convection cooling across rectangular blocks, *ASME J. Heat Transfer* **109,** 321–328 (1987).
17. J. S. Nigen and C. H. Amon, Forced convective cooling enhancement of surface-mounted electronic package configurations through self-sustained oscillatory flow, *ASME-HTD* **171,** 30–46 (1991).
18. S. H. Kim and N. K. Anand, Out flow boundary condition for temperature field in channels in presence of wall conduction, *Numer. Heat Transfer Part B* **25,** 163–176 (1994).
19. S. V. Patankar, *Numerical Heat Transfer and Fluid Flow*. Hemisphere, New York (1980).
20. H. S. Heaton, W. C. Reynolds and W. M. Kays, Simultaneous development of velocity and temperature fields in laminar flow, *Int. J. Heat Mass Transfer* **7,** 763–781 (1964).
21. R. E. Lundberg, W. C. Reynolds and W. M. Kays, Heat transfer with laminar flow in concentric annuli with constant and variable wall temperature and heat flux, NASA Technical Note TN D-1972.
22. B. W. Webb and S. Ramadhyani, Conjugate heat transfer in a channel with staggered ribs, *Int. J. Heat Mass Transfer* **28,** 1679–1687 (1985).
23. S. V. Patankar, C. H. Liu and E. M. Sparrow, Fully developed flow and heat transfer in ducts having streamwise-periodic variations of cross-sectional area, *ASME J. Heat Transfer* **99,** 180–186 (1977).